

Symmetry of shape charts

I. Ginkel, G. Umlauf*

Geometric Algorithms Group, Department of Computer Science, University of Kaiserslautern, D-67653 Kaiserslautern, Germany

Received 13 October 2006; received in revised form 23 February 2007; accepted 2 September 2007

Available online 14 September 2007

Abstract

For subdivision surfaces, the so-called shape chart can be used to characterize the curvature behavior at an extraordinary point a priori from the initial control net. Of late, it has been used in different approaches to tune subdivision algorithms to handle the so-called hybrid shapes. For this the shape charts are computed numerically. In this paper, symmetries of shape charts are analyzed that can be used to simplify the computations and to reduce the computation costs significantly.

© 2007 Elsevier B.V. All rights reserved.

Keywords: Subdivision surfaces; Shape charts

1. Introduction

Tuning has always been part of developing subdivision algorithms. The choice of suitable parameters for the first algorithms (Catmull and Clark, 1978; Loop, 1987) already improved the surfaces. Recently more sophisticated approaches that focus on shape improvement were made, see e.g. Barthe and Kobbelt (2004), Holt (1996), Loop (2003), Prautzsch and Umlauf (2000), Sabin (1991). Nevertheless, all these approaches lead to surfaces that still can have artifacts due to hybrid shapes (Karciauscas et al., 2004; Peters and Reif, 2004). This means that in any neighborhood of an extraordinary point positive and negative Gauss curvature might occur. To detect this behavior a priori the so-called shape charts (Karciauscas et al., 2004) can be used. They represent all possible shapes of surfaces a subdivision algorithm can generate in terms of the initial control net. Therefore, shape charts can also be used to tune subdivision algorithms.

In order to decrease the number of hybrid shapes in Augsdörfer et al. (2005, 2006) a tuning of the eigenvalues was used to minimize the variation of Gauss curvature near extraordinary points. Using this approach it is not possible to guarantee non-hybrid shapes. In Ginkel and Umlauf (2006a, 2006b) a technique is presented that can often avoid hybrid shapes. It consists of an eigenvalue and eigencoeficient tuning to allow for surfaces with bounded Gauss curvature of arbitrary constant sign. Thus, given an arbitrary initial control net an elliptic or a hyperbolic shape at the extraordinary points can be achieved, if there are non-hybrid points in the shape chart.

For both approaches the shape charts need to be computed numerically. This is computationally expensive limiting the accuracy of the computed shape charts. To enhance the computation of shape charts their symmetries can be

* Corresponding author.

E-mail addresses: ginkel@informatik.uni-kl.de (I. Ginkel), umlauf@informatik.uni-kl.de (G. Umlauf).

used to speed up the computation and improve their accuracy. Related results have independently been discovered by Hartmann (2005).

For this we recall in Section 2 the basic principles of subdivision analysis and sufficient conditions for subdivision algorithms with bounded curvature of arbitrary sign. In Section 3 the symmetry properties of the shape charts are presented, which allow a more efficient analysis of possible shape behavior.

2. Basic subdivision analysis techniques

For the standard analysis techniques consider a stationary, linear and symmetric subdivision algorithm generalizing box spline subdivision (Reif and Peters, 2006). In the neighborhood of an irregular vertex of valence $n \neq 6$ for triangular nets, a subdivision surface is the union of the extraordinary point \mathbf{q} and a sequence of spline rings \mathbf{x}_m , that are linear combinations of real valued functions $\varphi_0(s, t), \dots, \varphi_l(s, t)$ with control points $\mathbf{B}_m^0, \dots, \mathbf{B}_m^l \in \mathbb{R}^3$. Collecting the functions in a row vector $\boldsymbol{\varphi}(s, t)$ and the control points in a column vector \mathbf{B}_m we have $\mathbf{x}_m = \boldsymbol{\varphi} \mathbf{B}_m = \boldsymbol{\varphi} A^m \mathbf{B}_0$, where the sequence of control nets \mathbf{B}_m is generated by iterated multiplication of \mathbf{B}_0 with a square subdivision matrix A . It has eigenvalues $\lambda_0, \dots, \lambda_l$ with $|\lambda_0| \geq |\lambda_1| \geq \dots \geq |\lambda_l|$, corresponding to right eigenvectors $\mathbf{v}_0, \dots, \mathbf{v}_l$, and eigenfunctions $\psi_i(s, t) = \boldsymbol{\varphi}(s, t) \mathbf{v}_i$, which are the limit functions of \mathbf{v}_i under box spline subdivision. Then, the initial control net can be written as

$$\mathbf{B}_0 = \sum_{i=0}^l \mathbf{d}_i \mathbf{v}_i.$$

We assume that the $\mathbf{d}_1, \dots, \mathbf{d}_5$ are generic (Peters and Reif, 2004), i.e. $\det(\mathbf{d}_i, \mathbf{d}_j, \mathbf{d}_k) \neq 0$ for all sets $\{i, j, k\} \subset \{1, \dots, 5\}$.

For a symmetric subdivision algorithm A is block circulant (Reif and Peters, 2006) and can be transformed into a similar block diagonal matrix \hat{A} with diagonal blocks \hat{A}_k by a discrete Fourier transformation F

$$\hat{A} = F^{-1} A F = \text{diag}(\hat{A}_0, \dots, \hat{A}_{n-1}).$$

An eigenvalue $\nu \in \text{spec}(\hat{A}_k)$ is said to have *Fourier index* $\mathcal{F}(\nu) = k$. Then, sufficient conditions for regular subdivision surfaces to have continuous normal and bounded Gauss curvature of arbitrary sign are given by:

- (i) All rows of A sum to one, i.e. $\lambda_0 = 1 > |\lambda_1|$.
- (ii) The sub-dominant eigenvalue λ is positive and has algebraic and geometric multiplicity two $\lambda := \lambda_1 = \lambda_2 > |\lambda_3|$.
- (iii) The characteristic map $\Psi(s, t) := (\psi_1(s, t), \psi_2(s, t))$, which is the planar spline ring built from the sub-dominant eigenfunctions ψ_1, ψ_2 is injective and regular (Reif, 1995).
- (iv) The subsub-dominant eigenvalue μ satisfies $\mu = \lambda^2$.
- (v) The subsub-dominant eigenvalue $\mu = \lambda_3 = \lambda_4 = \lambda_5 > |\lambda_6|$ is positive and has equal algebraic and geometric multiplicity three with Fourier indices 0, 2 and $n - 2$ (Peters and Reif, 2004).

Condition (i) ensures convergence, (ii) and (iii) C^1 regularity, (iv) bounded curvature and (v) allows for arbitrary quadratic shapes. Unfortunately, the standard algorithms like the algorithm of Loop or Catmull/Clark do not meet these conditions and have to be modified accordingly Karciuscas et al. (2004).

To analyze higher order behavior of subdivision algorithms, the central surface depending on the initial control net is defined as the spline ring

$$\mathbf{x}_c := \left(\Psi L, \sum_{i=3}^5 \psi_i \langle \mathbf{d}_i, \mathbf{n} \rangle \right), \quad \mathbf{n} := (\mathbf{d}_1 \times \mathbf{d}_2) / \|\mathbf{d}_1 \times \mathbf{d}_2\|,$$

where L is the matrix that orthonormalizes $(\mathbf{d}_1, \mathbf{d}_2)$. Its Gauss curvature $K_{\mathbf{x}_c}(s, t)$ can be used to characterize, a priori, the behavior of the Gauss curvature of \mathbf{x} at an extraordinary point \mathbf{q} , see Peters and Reif (2004),

$$\mathbf{q} \text{ is } \begin{cases} \text{elliptic in the limit,} & \text{if } K_{\mathbf{x}_c}(s, t) > 0 \text{ for all } s, t, \\ \text{hyperbolic in the limit,} & \text{if } K_{\mathbf{x}_c}(s, t) < 0 \text{ for all } s, t, \\ \text{hybrid,} & \text{otherwise.} \end{cases}$$

Furthermore, for every \mathbf{q} the shape characteristic can be pre-computed. Expressing the third coordinate function ψ of \mathbf{x}_c in polar coordinates yields

$$\psi_{r,\vartheta} := \sum_{i=3}^5 \psi_i(\mathbf{d}_i, \mathbf{n}) = (1-r)\psi_3 + r \cos(\vartheta)\psi_4 + r \sin(\vartheta)\psi_5,$$

where $r \in [0, 1]$ and $\vartheta \in [0, 2\pi]$. Without loss of generality this allows only for central surfaces with the same orientation. This can be achieved by

$$r = \frac{\sqrt{\langle \mathbf{d}_4, \mathbf{n} \rangle^2 + \langle \mathbf{d}_5, \mathbf{n} \rangle^2}}{\sqrt{\langle \mathbf{d}_4, \mathbf{n} \rangle^2 + \langle \mathbf{d}_5, \mathbf{n} \rangle^2 + \langle \mathbf{d}_3, \mathbf{n} \rangle^2}}, \quad \vartheta = \arccos \frac{\langle \mathbf{d}_4, \mathbf{n} \rangle}{\sqrt{\langle \mathbf{d}_4, \mathbf{n} \rangle^2 + \langle \mathbf{d}_5, \mathbf{n} \rangle^2}},$$

which implies a different scaling of $\mathbf{v}_3, \mathbf{v}_4, \mathbf{v}_5$ for every point in the shape chart. Denote by $K_{r,\vartheta}(s, t)$ the Gauss curvature of the central surface \mathbf{x}_c defined by (r, ϑ) at parameter (s, t) . Then, the *shape chart map* \mathbf{s} is defined as

$$\mathbf{s}(r, \vartheta) = \begin{cases} 0 & \text{if } K_{r,\vartheta}(s, t) < 0 \text{ for all } s, t, \\ 1 & \text{if } K_{r,\vartheta}(s, t) > 0 \text{ for all } s, t, \\ \frac{1}{2} & \text{otherwise.} \end{cases}$$

The mapping of $\mathbf{s}(r, \vartheta)$ to the colors blue, red and green yields the so-called *shape chart* (Karciauscas et al., 2004). Examples of shape charts are shown in Figs. 1 and 2.¹

3. Properties of the shape charts

To enhance the computation of the shape charts its rotational and mirror symmetries can be utilized.

First we analyze the regular case. For a regular control net the control points of the one-ring of the characteristic map for the algorithm of Loop form a regular 6-gon. So, due to linear precision, the characteristic map is linear and the central surface is quadratic, since subdivision of quartic box splines yields C^2 surfaces (Prautzsch and Reif, 1999). For a quadratic polynomial function the Gauss curvature has a constant sign, because $\mathbf{L} \cdot \mathbf{N} - \mathbf{M}^2$ is constant, where $\mathbf{L}, \mathbf{M}, \mathbf{N}$ represent the second fundamental form. Thus, to find the shape chart characterization it suffices to evaluate the curvature of the central surface at an arbitrary parameter.

Theorem 1. For box spline subdivision with directions $\begin{bmatrix} 1 & 1 & 0 & 0 & 1 & 1 \\ 0 & 0 & 1 & 1 & 1 & 1 \end{bmatrix}$ all central surfaces with $K_{r,\vartheta} \equiv 0$ correspond to a constant r .

Proof. For these box spline the eigenfunctions are given by $\psi_1(s, t) = s, \psi_2(s, t) = t, \psi_3(s, t) = \frac{1}{2}(s^2 + t^2), \psi_4(s, t) = \frac{1}{2}(s^2 - t^2)$ and $\psi_5(s, t) = st$, which are only unique up to scaling. Scaling such that $\psi_3(s, t) \in [0, 1]$ and $\psi_4(s, t) + \psi_5(s, t) \in [-1, 1]$ for $s, t \in [-1, 1]$, yields for the third coordinate function ψ of the central surfaces at (s, t)

$$\psi_{r,\vartheta} = (1-r)\frac{1}{2}(s^2 + t^2) + r \cos(\vartheta)\frac{1}{2}(s^2 - t^2) + r \sin(\vartheta)st.$$

So, at the origin the second fundamental form is $\mathbf{L} = 1 - r - r \cos(\vartheta), \mathbf{M} = r \sin(\vartheta), \mathbf{N} = 1 - r + r \cos(\vartheta)$. Solving $\mathbf{L} \cdot \mathbf{N} - \mathbf{M}^2 = 0$ for r , yields $r = \frac{1}{2}$.

Remark 2. For an arbitrary subdivision algorithm, which generates C^2 surfaces for regular nets, a linear characteristic map implies that no hybrid shapes are created for points corresponding to regular vertices. This is consistent with the fact that the surfaces are C^2 in these points.

For subdivision algorithms for meshes with irregular vertices the area in the shape chart of parabolic configurations is in general not a circle, but the respective shape charts still have similar symmetry properties.

¹ For interpretation of the references to color, the reader is referred to the web version of this article.

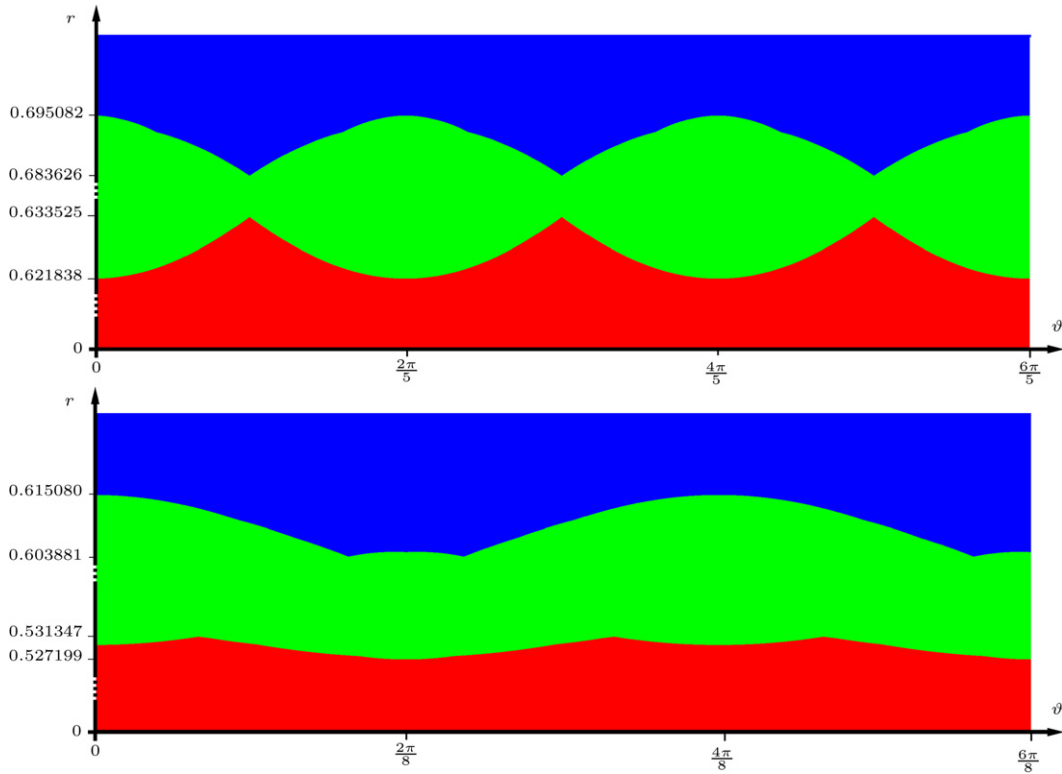


Fig. 1. Three segments of shape charts for the modified algorithm of Loop in Ginkel and Umlauf (2006b) for $n = 5$ (top) and $n = 8$ (bottom).

Theorem 3. For a symmetric subdivision algorithm the shape chart map \mathbf{s} is rotationally and mirror symmetric, i.e.

$$\mathbf{s}\left(r, \frac{2\pi k}{n} + \vartheta\right) = \mathbf{s}(r, \vartheta) \quad \text{for } \begin{cases} k \in \mathbb{N}_0, & \text{if } n \text{ is odd,} \\ k \in 2\mathbb{N}_0, & \text{if } n \text{ is even,} \end{cases} \quad (1)$$

$$\mathbf{s}\left(r, \frac{2\pi k}{n} + \vartheta\right) = \mathbf{s}\left(r, \frac{2\pi k}{n} - \vartheta\right) \quad \text{for } \begin{cases} k \in \frac{1}{2}\mathbb{N}_0, & \text{if } n \text{ is odd,} \\ k \in \mathbb{N}_0, & \text{if } n \text{ is even.} \end{cases} \quad (2)$$

Proof. To prove (2) compare the ranges of $K_{r, 2\pi k/n + \vartheta}$ and $K_{r, 2\pi k/n - \vartheta}$. The control points of the respective central surfaces are defined by the eigenvectors $\mathbf{v}_1, \dots, \mathbf{v}_5$ and the polar coordinates of the respective point in the shape chart. The abscissae of these control points are those of the characteristic map Ψ which is rotationally and mirror symmetric, because $\mathcal{F}(\lambda) \in \{1, n - 1\}$ and the subdivision algorithm is assumed to be symmetric. Furthermore, the eigenvector \mathbf{v}_3 has Fourier index 0, i.e. ψ_3 is the same for every segment and it is rotationally and mirror symmetric. Thus, it suffices to analyze the hyperbolic components of ψ depending only on ψ_4 and ψ_5 . Denote by $\hat{\mathbf{v}}$ the eigenvector of \hat{A}_2 corresponding to μ , then \mathbf{v}_4 and \mathbf{v}_5 are given as the real and imaginary parts of $[\hat{\mathbf{v}}^t, \omega^2 \hat{\mathbf{v}}^t, \dots, \omega^{2(n-1)} \hat{\mathbf{v}}^t]^t$, with $\omega = \exp(2\pi\sqrt{-1}/n)$. This yields for the hyperbolic components of ψ

$$\begin{aligned} & \cos\left(\frac{2\pi k}{n} + \vartheta\right)\psi_4 + \sin\left(\frac{2\pi k}{n} + \vartheta\right)\psi_5 \\ &= \varphi \begin{bmatrix} \cos\left(\frac{2\pi k}{n} + \vartheta - 0 \cdot \frac{4\pi}{n}\right) \text{Re}(\hat{\mathbf{v}}) + \sin\left(\frac{2\pi k}{n} + \vartheta - 0 \cdot \frac{4\pi}{n}\right) \text{Im}(\hat{\mathbf{v}}) \\ \vdots \\ \cos\left(\frac{2\pi k}{n} + \vartheta - (n-1) \cdot \frac{4\pi}{n}\right) \text{Re}(\hat{\mathbf{v}}) + \sin\left(\frac{2\pi k}{n} + \vartheta - (n-1) \cdot \frac{4\pi}{n}\right) \text{Im}(\hat{\mathbf{v}}) \end{bmatrix} \end{aligned}$$

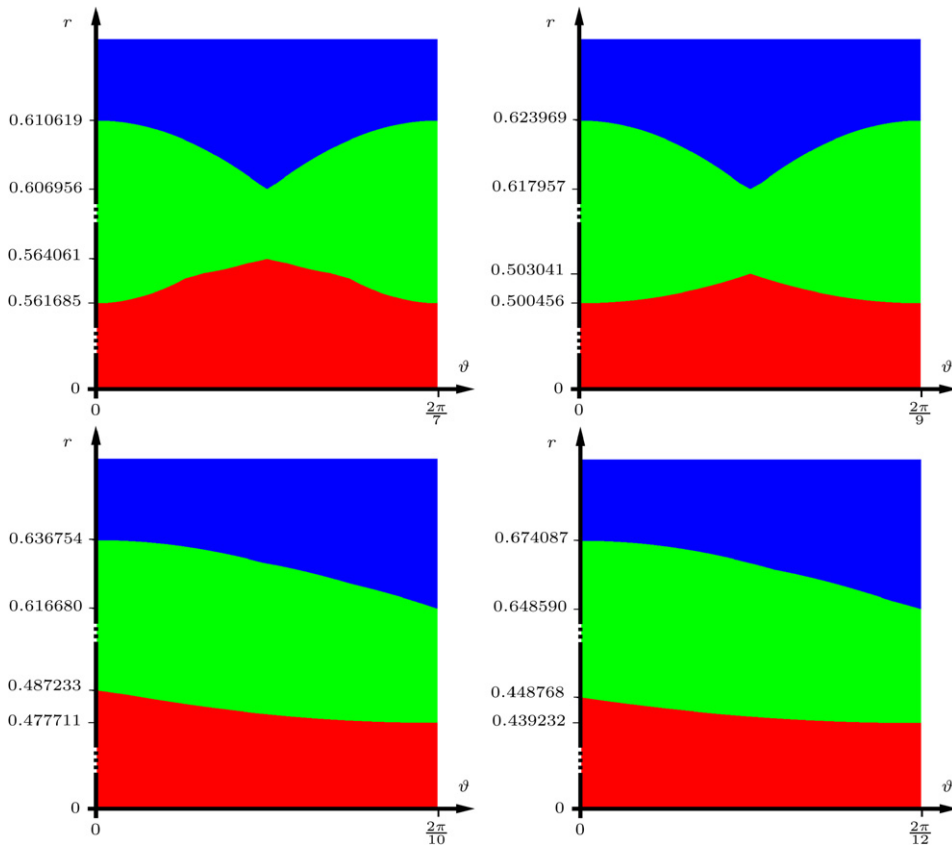


Fig. 2. Single segments of shape charts for the modified algorithm of Loop in Ginkel and Umlauf (2006b) for $n = 7$ (top left), $n = 9$ (top right), $n = 10$ (bottom left) and $n = 12$ (bottom right).

$$\begin{aligned}
 &= \varphi \begin{bmatrix} \cos\left(\frac{2\pi k}{n} - \vartheta + (0 - k) \cdot \frac{4\pi}{n}\right) \operatorname{Re}(\hat{\mathbf{v}}) - \sin\left(\frac{2\pi k}{n} - \vartheta + (0 - k) \cdot \frac{4\pi}{n}\right) \operatorname{Im}(\hat{\mathbf{v}}) \\ \vdots \\ \cos\left(\frac{2\pi k}{n} - \vartheta + (n - 1 - k) \cdot \frac{4\pi}{n}\right) \operatorname{Re}(\hat{\mathbf{v}}) - \sin\left(\frac{2\pi k}{n} - \vartheta + (n - 1 - k) \cdot \frac{4\pi}{n}\right) \operatorname{Im}(\hat{\mathbf{v}}) \end{bmatrix} \\
 &= \cos\left(\frac{2\pi k}{n} - \vartheta\right) \varphi \operatorname{Re} \begin{bmatrix} \omega^{-2(0-k)} \hat{\mathbf{v}} \\ \vdots \\ \omega^{-2(n-1-k)} \hat{\mathbf{v}} \end{bmatrix} + \sin\left(\frac{2\pi k}{n} - \vartheta\right) \varphi \operatorname{Im} \begin{bmatrix} \omega^{-2(0-k)} \hat{\mathbf{v}} \\ \vdots \\ \omega^{-2(n-1-k)} \hat{\mathbf{v}} \end{bmatrix}.
 \end{aligned}$$

Due to Reif and Peters (2006, Section 6) this is a mirroring of the indexing of the control points. So, the ordinates of the central surfaces are mirrored and the range of the curvature of the central surfaces does not change. So, (2) follows for all n and $k \in \mathbb{N}_0$. Since two successive mirrorings equal a rotation, (1) follows for arbitrary n and even k . Rotating by more than 2π , yields (1) for odd n and arbitrary $k \in \mathbb{N}_0$ and (2) for odd n and $k \in \frac{1}{2}\mathbb{N}_0$. \square

Thus, to compute a shape chart one segment $\vartheta \in [0, 2\pi/n]$ for even valences and half a segment $\vartheta \in [0, \pi/n]$ for odd valences suffices. Examples for the modified algorithm of Loop in Ginkel and Umlauf (2006b) of three segments of the shape charts for $n = 5$ and $n = 8$ are shown in Fig. 1 to emphasize the different symmetries. In Fig. 2 single segments of the shape charts for $n \in \{7, 9, 10, 12\}$ are shown.

The hybrid areas in Figs. 1 and 2 grow with the valence. For high valences the hybrid area covers the complete shape chart. For example the central surfaces $(\Psi L, \psi_3)$ and $(\Psi L, \psi_4)$ for the modified algorithm of Loop in Ginkel and Umlauf (2006b) have hybrid curvature behavior for high valences, see Fig. 3. We checked the sign of the curvature also symbolically for $(\Psi L, \psi_3)$ for $n = 64$ and for $(\Psi L, \psi_4)$ for $n = 24$. In both cases a change of sign proved the hybrid behavior.

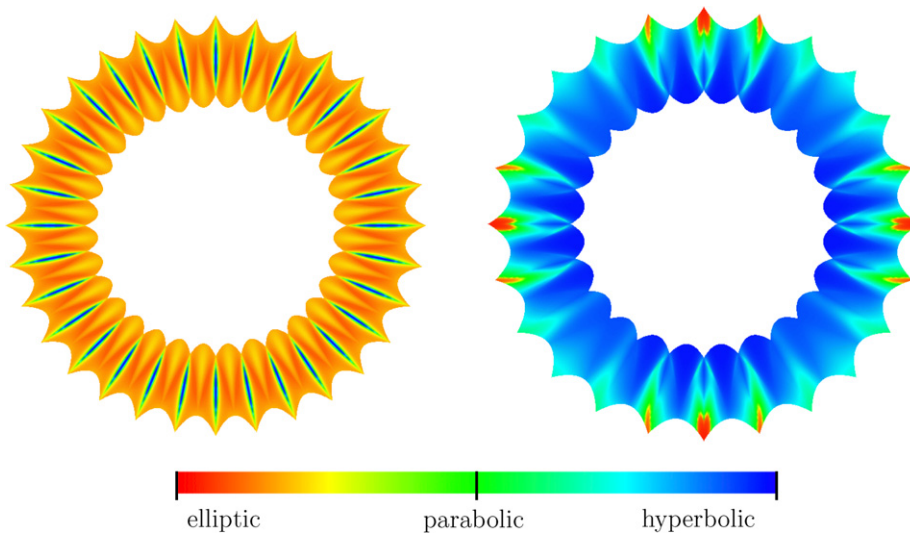


Fig. 3. Hybrid central surfaces $(\Psi L, \psi_3)$ ($n = 32$, $\mathcal{F}(\mu) = 0$, left) and $(\Psi L, \psi_4)$ ($n = 24$, $\mathcal{F}(\mu) = 2$, right) of the modified algorithm of Loop in Ginkel and Umlauf (2006b).

Acknowledgements

The authors would like to thank Jörg Peters and the anonymous reviewers for their helpful comments.

References

- Augsdörfer, U., Dodgson, N.A., Sabin, M.A., 2005. A new way to tune subdivision. In: Desbrun, M., Pottmann, H. (Eds.), Eurographics Symposium on Geometry Processing.
- Augsdörfer, U., Dodgson, N.A., Sabin, M.A., 2006. Tuning subdivision by minimising the Gaussian curvature variation near extraordinary vertices. In: Gröller, E., Szirmay-Kalos, L. (Eds.), Proc. Eurographics.
- Barthe, L., Kobbelt, L., 2004. Subdivision scheme tuning around extraordinary vertices. *Comput. Aided Geom. Design* 21 (6), 561–583.
- Catmull, E., Clark, J., 1978. Recursive generated b-spline surfaces on arbitrary topological meshes. *Computer-Aided Design* 10, 350–355.
- Ginkel, I., Umlauf, G., 2006a. Controlling a subdivision tuning method. In: Cohen, A., Merrien, J.-L., Schumaker, L.L. (Eds.), *Curve and Surface Fitting*. Avignon 2006. Nashboro Press, pp. 170–179.
- Ginkel, I., Umlauf, G., 2006b. Loop subdivision with curvature control. In: Polthier, K., Sheffer, A. (Eds.), *Symposium on Geometry Processing*. Eurographics Association, pp. 163–172.
- Hartmann, R., 2005. *Formeigenschaften von Subdivisions-Algorithmen*. Master's thesis, Technische Universität Darmstadt (in German).
- Holt, F., 1996. Towards a curvature continuous stationary subdivision algorithm. *Z. Angew. Math. Mech.* 76, 423–424.
- Karciauskas, K., Peters, J., Reif, U., 2004. Shape characterization of subdivision surfaces—case studies. *Comput. Aided Geom. Design* 21 (6), 601–614.
- Loop, C., 1987. *Smooth subdivision surfaces based on triangles*. Master's thesis, University of Utah.
- Loop, C., 2003. Smooth ternary subdivision of triangle meshes. In: Cohen, A., Merrien, J.-L., Schumaker, L.L. (Eds.), *Curve and Surface Fitting*. Saint-Malo 2002. Nashboro Press, pp. 295–302.
- Peters, J., Reif, U., 2004. Shape characterization of subdivision surfaces—basic principles. *Comput. Aided Geom. Design* 21 (6), 585–599.
- Prautzsch, H., Reif, U., 1999. Degree estimates for C^k -piecewise polynomial subdivision surfaces. *Adv. Comput. Math.* 10 (2), 209–217.
- Prautzsch, H., Umlauf, G., 2000. A G^1 and a G^2 subdivision scheme for triangular nets. *Int. J. Shape Modeling* 6 (1), 21–35.
- Reif, U., 1995. A unified approach to subdivision algorithms near extraordinary vertices. *Comput. Aided Geom. Design* 12, 153–174.
- Reif, U., Peters, J., 2006. Structural analysis of subdivision surfaces—a summary. In: Jetter, K., et al. (Eds.), *Topics in Multivariate Approximation and Interpolation*. Elsevier, pp. 149–190.
- Sabin, M.A., 1991. Cubic recursive division with bounded curvature. In: Laurent, P.J., Le Méhauté, A., Schumaker, L.L. (Eds.), *Curves and Surfaces* pp. 411–414.